Generation of Phase-Locked Pulses from a Seeded Free-Electron Laser

David Gauthier,[1,*] Primož Rebernik Ribič,[1] Giovanni De Ninno,[1,2] Enrico Allaria,[1] Paolo Cinquegrana,[1] Miltcho Bojanov Danailov,[1] Alexander Demidovich,[1] Eugenio Ferrari,[1,3] and Luca Giannessi[1,4]
[1]*Elettra-Sincrotrone Trieste, Strada Statale 14-km 163,5, 34149 Basovizza, Trieste, Italy*
[2]*Laboratory of Quantum Optics, University of Nova Gorica, 5001 Nova Gorica, Slovenia*
[3]*Università degli Studi di Trieste, Dipartimento di Fisica, Piazzale Europa 1, 34100 Trieste, Italy*
[4]*Theory Group ENEA Frascati, Via Enrico Fermi 45, 00044 Frascati, Italy*
(Received 13 November 2015; published 14 January 2016)

In a coherent control experiment, light pulses are used to guide the real-time evolution of a quantum system. This requires the coherence and the control of the pulses' electric-field carrier waves. In this work, we use frequency-domain interferometry to demonstrate the mutual coherence of time-delayed pulses generated by an extreme ultraviolet seeded free-electron laser. Furthermore, we use the driving seed laser to lock and precisely control the relative phase between the two free-electron laser pulses. This new capability opens the way to a multitude of coherent control experiments, which will take advantage of the high intensity, short wavelength, and short duration of the pulses generated by seeded free-electron lasers.

DOI: 10.1103/PhysRevLett.116.024801

Ultrafast light-matter interaction in the UV to x-ray spectral domain is a rich research field ranging from fundamental to applied physics, and from chemistry to biology and materials science. Because of the constant progress, there is a strong need for further technological improvements in the area of new coherent light sources. Quantum coherent control, coherent nonlinear optics, and multidimensional spectroscopy [1–3] are examples of topics which require powerful and coherent multiple extreme ultraviolet (XUV) pulses, with complete control of the light properties, such as the wavelength, timing, and even the relative phase between the electric-field carrier waves.

The common approach to create time-delayed multiple pulses is to employ an interferometric setup acting directly on the XUV beam. Because of the difficulties of manufacturing transmission optics and beam splitters for short wavelengths [4], most of the interferometers are based on diffractive optics [5] or, more generally, on the use of a wave-front division system [6,7], particularly for free-electron lasers (FELs) [8,9]. A second possible approach is to *directly* generate pulses with the required properties. This is possible on laser-driven sources by using an interferometer on the generating laser, where the optical and mechanical constraints are relaxed. These XUV sources generally inherit the coherence properties of the driving laser and, therefore, have the capability to generate phase-locked XUV pulses. The principle was demonstrated for the so-called high harmonic generation [10–12] and used in various experiments [13–15].

In the last years, significant effort has been devoted to generation of multiple pulses with controllable time delays and/or wavelengths using different configurations on single-pass FELs [16–22]. However, the mutual coherence between the pulses is not considered or not directly characterized. Only recently, the first demonstration of a coherent control experiment was performed [23]. By controlling the relative phase between two time-overlapped pulses with commensurate wavelengths, it was possible to guide the ionization pathways in neon. However, the configuration was limited to time-independent studies.

In this work, we make use of *frequency-domain* interferometry to demonstrate the generation of two time-delayed phase-locked XUV pulses from a seeded FEL. We show the possibility of controlling the phase difference between the carrier waves of the two pulses. The generation and control of multiple mutually coherent pulses represents an important step forward beyond the generation of multiple uncorrelated coherent pulses in seeded FELs. This capability could allow us, for example, to perform *temporal* coherent control experiments for guiding the real-time evolution of a quantum system [24–26] and this with femtosecond powerful short-wavelength light pulses. It also constitutes the first step to a multitude of nonlinear coherent transient interferometric and spectroscopic methods with x rays, e.g., Ramsey interferometry, "photon echo," and spectral holography using core-level spectral hole burning [27,28].

The experiment was performed at the FERMI FEL facility [29,30] and exploits the capability of the seed laser to trigger and drive the FEL process and generate coherent and controllable XUV pulses. The original purpose of seeding a FEL to initiate light emission, as, for example, in the high gain harmonic generation (HGHG) configuration [31], was to improve the longitudinal coherence with respect to the self-amplified spontaneous emission FEL. However, a few theoretical [32] and recent experimental [33,34] works show that one can go beyond this idea and

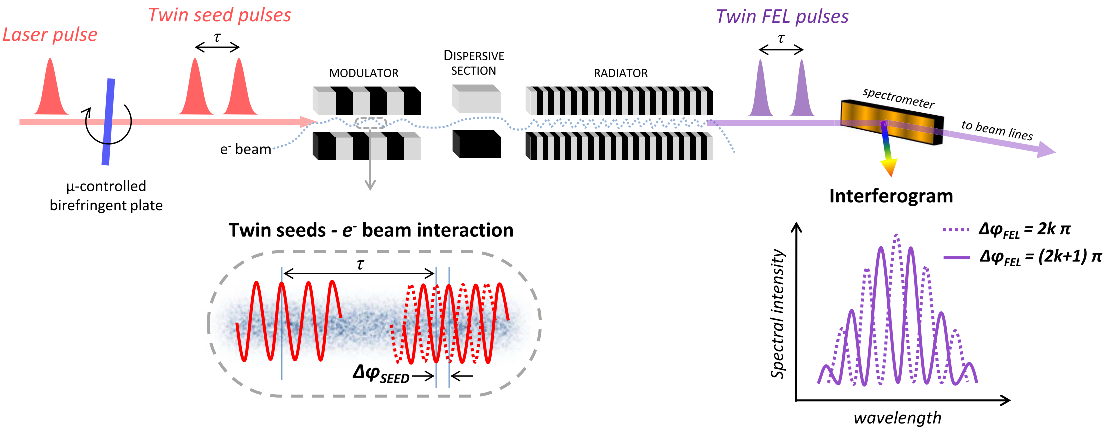

FIG. 1. HGHG FEL in the two phase-locked pulses configuration. Two time-delayed seed pulses are created by transmission of a single laser pulse through a birefringent plate. The plate is motorized to precisely control the relative phase $\Delta\varphi_{\mathrm{seed}}$ between the two carrier waves of the twin seeds, which interact with the relativistic electron beam in the modulator. The time-delayed twin FEL pulses are spectrally overlapped and give rise to a spectral interference pattern acquired by an online spectrometer. The relative phase $\Delta\varphi_{\mathrm{FEL}}$ can be deduced from the distribution of the fringes in the interferogram. As an example, two cases are sketched (with k integer). For the experiment reported here, $\tau = 280$ fs, and the estimated duration of the individual FEL pulse is about 70–80 fs.

that the FEL pulse can be controlled by the seed laser and by tuning the FEL operating parameters. Figure 1 shows the experimental setup for the generation of two time-delayed phase-locked pulses implemented at FERMI. The twin seed pulses are produced from a single pulse (the third harmonic of a Ti:sapphire laser, $\lambda_{\mathrm{seed}} = 261.5$ nm) and temporally split into two pulses by transmission through a birefringent plate. The plate thickness and the group velocity difference for the two orthogonal axes of the birefringent plate rotated at 45° with respect to the laser polarization determine the time delay τ between the two seed pulses. Then, both polarization components are projected onto the interaction axis of the modulator. The relative phase between the carrier waves of the twin seed pulses $\Delta\varphi_{\mathrm{seed}}$ is controlled by fine-tuning the incidence angle on the plate. This is done by rotating the plate using a μ-controlled motorized rotation stage. The calculated minimum phase step that can be achieved is about 0.2 rad and is limited by the motor resolution. The two seeds interact with the relativistic electron beam inside the modulator and give rise to a periodic energy modulation at the seed wavelength, which is confined to the position of the two seed pulses within the electron beam (see Fig. 1). The relativistic electron beam comes from a linear accelerator (LINAC), where it was accelerated to an energy of 1014 MeV for the present experiment. The current profile of the electron beam is flat at around 550 amps, with a duration of about 1 ps, and a homogeneous time-dependent energy profile (see the Supplemental Material [35]). The energy modulation from the interaction between the electron beam and the twin seed pulses is converted into a periodic charge density modulation (microbunching) after the dispersive section. The microbunching triggers the emission of coherent light at one of the seed harmonics, which is then amplified in the radiator. Finally, the two output FEL pulses are sent to the beam line end station, and single-shot spectra are recorded by an online spectrometer [38].

Two mutually coherent pulses delayed in time produce a spectral interference pattern [39]. This configuration is the temporal equivalent of the Young's double slit interferometer, the time-delayed pulses playing the role of the spatially separated slits, and the spectrometer being the equivalent of the far-field screen, where the interference arises in the frequency domain. In the resulting interferogram, the fringe spacing is inversely proportional to the time delay, and the interferogram envelope is a superposition of the spectral envelopes of the two individual pulses. The fringe distribution within the interferogram contains information on the spectral phase difference of the two interfering pulses, a key parameter in all interferometric methods. For identical interfering pulses, the fringe contrast is maximal with a regular distribution of the fringes within the interferogram. Except for the relative phase, any additional variation of the temporal profile of the two pulses creates a difference between their amplitude and phase profiles in the frequency domain, with a tendency to reduce the contrast and complicate the fringe pattern. In the experiment, we were interested in the control of the fringe position inside the interferogram envelope, which is directly related to the control of the phase difference $\Delta\varphi_{\mathrm{FEL}}$ between the two FEL pulses. In the ideal case, for a homogeneous and symmetric interferogram, the relative phase between the two interfering pulses is obtained from the position of the fringes as sketched in Fig. 1. In the general case, the evolution of the relative phase can be deduced from the shift of the fringe pattern inside the interferogram envelope: a phase change of π induces a displacement equal to half of the fringe spacing, while 2π (one wavelength) results in a displacement identical to the fringe spacing. This is a well-known property of interferometric methods which are highly sensitive to the phase.

Because the seed laser produces the microbunching, the FEL emission initiated by this coherent structure of electrons is expected to reflect the seed properties. We, therefore, expect that the two FEL pulses obtained using the above scheme are mutually coherent and that their phase can be precisely controlled. The relative phase between the two FEL pulses is related to the one between the two seeds according to

$$\Delta\varphi_{\mathrm{FEL}} = n \times \Delta\varphi_{\mathrm{seed}} + C, \qquad (1)$$

where the FEL emission occurs at the nth ($n = 5$ for the data shown) harmonic of the seed wavelength. C includes the phase contribution related to the electron beam time-dependent energy profile [35], and a possible phase difference developed during pulse amplification in the radiator. We will see in the following that, although ideally constant, C might vary shot to shot due to different sources of phase instability. Figure 2(a) shows the evolution of the spectral fringes as a function of the μ-controlled rotation angle of the birefringent plate. Rotating the plate by 68 motor steps, we changed the relative phase between the twin seeds by $\Delta\varphi_{\mathrm{seed}} = 2.4 \times \lambda_{\mathrm{seed}}$ ($=2.4 \times 2\pi$ rad, one wavelength being equivalent to 2π rad) corresponding to a relative phase change of $\Delta\varphi_{\mathrm{FEL}} = 12 \times \lambda_{\mathrm{FEL}}$ for the two FEL pulses. From these numbers, we deduce a minimum step size of $\lambda_{\mathrm{seed}}/28.33$ corresponding to $\lambda_{\mathrm{FEL}}/5.67$. Figures 2(b) and 2(c) highlight the fringe displacement for each motor step. The ability to control the fringe displacement confirms that the phase relationship existing between the twin seed pulses is transferred onto the two FEL pulses. This is a direct consequence of the principle on which a seeded FEL working in the harmonic generation configuration relies.

The analysis of a sequence of shot-to-shot interferograms for a fixed motor position contains complementary information on the stability of the phase locking. More generally, the shot-to-shot regularity of the interferogram indicates that the relative amplitude and phase profile of the pulses are conserved. A sequence of 2000 single-shot spectra without changing the relative phase between the twin seed pulses is shown in Fig. 3(a). Figure 3(b) highlights the profiles of ten single-shot interferograms extracted from Fig. 3(a). The statistics on the shot-to-shot stability of the position of a central fringe is shown in the histogram in Fig. 3(c). The fringe stability is about FS/2 peak to valley and FS/12 rms, where FS is the fringe spacing equal to 0.0372 nm. From this, we deduce a phase stability of about $\pi/6$ rad ($\lambda_{\mathrm{FEL}}/12$) rms, which corresponds to temporal fluctuations lower than 15 attosecond between the carrier waves of two consecutive FEL pulses. Notice that the measured fringe instabilities are a consequence of different effects, including the instability of the seed laser itself and possible detection problems due to the variation of the FEL beam pointing on the spectrometer

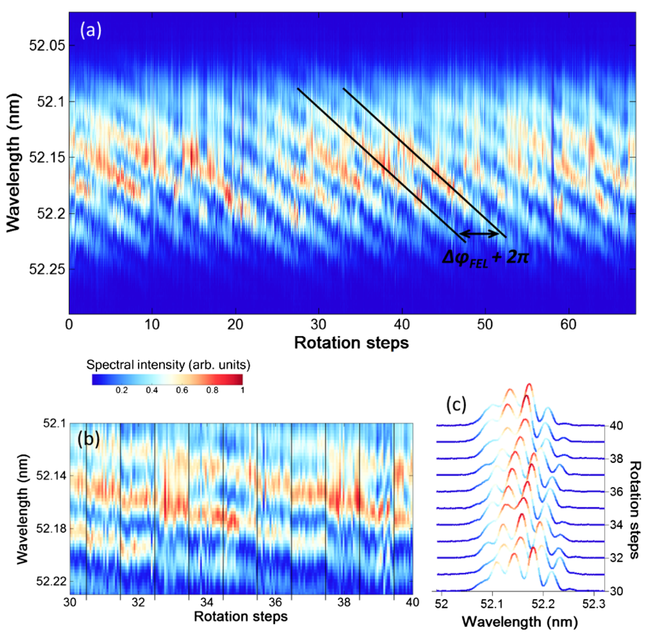

FIG. 2. Interferogram from two phase-locked FEL pulses. (a) Evolution of the spectral interference fringes as a function of the μ-controlled rotation angle of the birefringent plate (see Fig. 1). (b) Zoom of the central part. At each rotation step, 20 consecutive single-shot spectra are acquired. (c) Single-shot profiles extracted from (b), one for each rotation step.

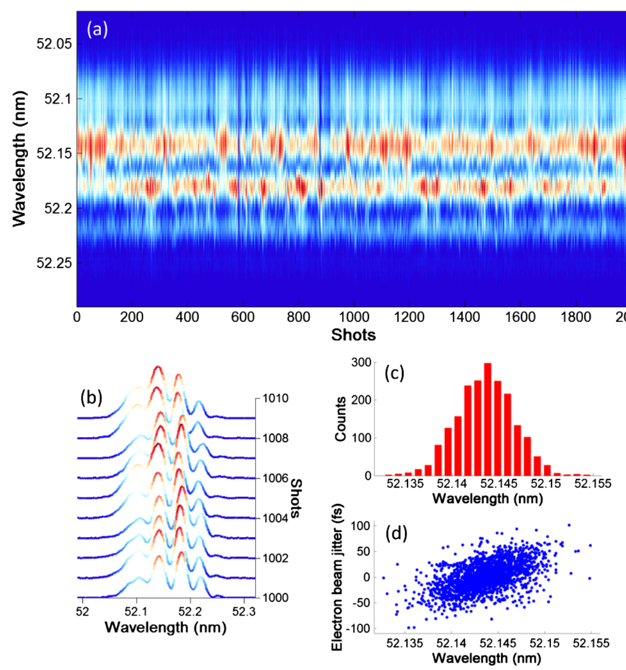

FIG. 3. Analysis of the fringe stability. (a) Sequence of 2000 spectra acquired for a fixed angle of the birefringent plate. (b) Ten single-shot interferogram profiles extracted from (a). (c) Histogram showing the distribution of the position of a central fringe on the spectrometer. (d) Correlation between the fringe position and the electron beam temporal jitter.

(the latter is not related to the phase instability). However, the main source of fringe instability is associated with the longitudinal properties of the electron beam, as highlighted, for example, by the correlation between the fringe displacement and the electron beam temporal jitter [Fig. 3(d)].

In a FEL, the light is emitted by relativistic electrons wiggling inside a periodic and static magnetic field produced by an undulator [40]. Consequently, the properties of the electron beam are expected to influence the characteristics of the emitted light and will compete with the ones driven by the seed laser. During acceleration in the LINAC, the e^- beam acquires a time-dependent energy profile [41]. In the case of the FERMI FEL, the length of the electron beam is compressed in time by a magnetic bunch compressor. Amplitude and phase fluctuations in the radio-frequency accelerating cavities before the bunch compressor give rise to a time jitter together with variations of the time-dependent energy profile of the e^- beam. Moreover, acceleration and compression in the LINAC result in a longitudinal instability called the microbunching instability [42]. All these effects have a double impact in our experiment. First, because the two time-delayed seed pulses see different parts of the time-dependent electron beam energy profile (see the Supplemental Material [35]), and due to additional pulse inhomogeneities coming from the microbunching instability, the FEL produces nonidentical pulses, which results in a reduced fringe contrast [see Figs. 2(c) and 3(b)]. Second, the variation of the e^- beam energy profile together with a time jitter between the twin seeds and the e^- beam [43] are the main sources of the fringe instabilities shown in Fig. 3. These effects are mostly related to the influence of the time-dependent energy profile on the temporal phase of each FEL pulse [37,44] and, consequently, on the relative phase difference between them [term C in Eq. (1)] [35]. Notice that any relative evolution of the amplitude and phase profiles between the pulses will induce a response on their spectral interference pattern. Therefore, important statistical information on the pulse evolution and stability is also encoded in the spectral fringe distribution. Because of this fact, the interferometric method could be a valuable tool for monitoring the FEL stability and performance. Finally, the stability reported here can be substantially improved by reducing the dependence on the e^- beam characteristics. This will be achieved at FERMI in the short term with the linearization of the time-dependent energy profile of the e^- beam [41].

In conclusion, using an interferometric setup, we demonstrated phase locking between two pulses from a seeded FEL and studied the control and the stability of their relative temporal properties. It turned out that the physical process on which a FEL relies preserves the mutual coherence driven by the two seed laser pulses. Finally, we identified the nonideal electron beam as the main source of the remaining phase instability. In the general context of laser-driven light sources, we demonstrated the capability to control and manipulate the light emitted by a seeded FEL [33,45]. The setup reported in this Letter is very flexible because the seed laser can be easily upgraded to various configurations. For example, by extending the FEL output from two to a train of multiple phase-locked pulses, a frequency comblike spectrum could be generated [46,47]. Moreover, the individual control of each pulse, specifically its spectral phase, opens the door to a vast range of coherent control applications at short wavelengths, such as quantum state holography [48]. The generation of phase-locked pulses will be naturally available for photon energies in the soft x-ray spectral region using the FERMI two-stage HGHG FEL [30] and an extension to self-seeding schemes operating in the x-ray regime might be envisaged [21].

We acknowledge the assistance of the entire FERMI team during the preparation and tuning of the FEL and particularly the contribution of S. Di Mitri, G. Gaio, G. Penco, and E. Roussel. We thank the laser group of FERMI and the PADReS group for the support on the photon diagnostics. We also acknowledge useful discussions with B. Mahieu and W. M. Fawley.

[*]david.gauthier@elettra.eu

[1] B. W. Adams *et al.*, X-ray quantum optics, J. Mod. Opt. **60**, 2 (2013).

[2] S. T. Cundif and S. Mukamel, Optical multidimensional coherent spectroscopy, Phys. Today **66**, 44 (2013).

[3] I. V. Schweigert and S. Mukamel, Double-quantum-coherence attosecond x-ray spectroscopy of spatially separated, spectrally overlapping core-electron transitions, Phys. Rev. A **78**, 052509 (2008).

[4] F. Delmotte, M.-F. Ravet, F. Bridou, F. Varnière, P. Zeitoun, S. Hubert, L. Vanbostal, and G. Soullie, X-ray ultraviolet beam splitters for the Michelson interferometer, Appl. Opt. **41**, 5905 (2002).

[5] S. Chakrabarti, D. M. Cotton, J. S. Vickers, and B. C. Bush, Self-compensating, all-reflection interferometer, Appl. Opt. **33**, 2596 (1994).

[6] P. Tzallas, E. Skantzakis, L. A. A. Nikolopoulos, G. D. Tsakiris, and D. Charalambidis, Extreme-ultraviolet pump probe studies of one-femtosecond-scale electron dynamics, Nat. Phys. **7**, 781 (2011).

[7] N. de Oliveira, M. Roudjane, D. Joyeux, D. Phalippou, J.-C. Rodier, and L. Nahon, High-resolution broad-bandwidth Fourier-transform absorption spectroscopy in the VUV range down to 40 nm, Nat. Photonics **5**, 149 (2011).

[8] Y. H. Jiang *et al.*, Temporal coherence effects in multiple ionization of N_2 via XUV pump-probe autocorrelation, Phys. Rev. A **82**, 041403 (2010).

[9] F. Bencivenga *et al.*, Four-wave mixing experiments with extreme ultraviolet transient gratings, Nature (London) **520**, 205 (2015).

[10] R. Zerne, C. Altucci, M. Bellini, M. B. Gaarde, T. W. Hänsch, A. L'Huillier, C. Lyngå, and C.-G. Wahlström, Phase-Locked High-Order Harmonic Sources, Phys. Rev. Lett. **79**, 1006 (1997).

[11] P. Salières, L. Le Déroff, T. Auguste, P. Monot, P. d'Oliveira, D. Campo, J.-F. Hergott, H. Merdji, and B. Carré, Frequency-Domain Interferometry in the XUV with High-Order Harmonics, Phys. Rev. Lett. **83**, 5483 (1999).

[12] M. Kovacev *et al.*, Extreme Ultraviolet Fourier-Transform Spectroscopy with High Order Harmonics, Phys. Rev. Lett. **95**, 223903 (2005).

[13] S. Cavalieri, R. Eramo, M. Materazzi, C. Corsi, and M. Bellini, Ramsey-Type Spectroscopy with High-Order Harmonics, Phys. Rev. Lett. **89**, 133002 (2002).

[14] T. Remetter *et al.*, Attosecond electron wave packet interferometry, Nat. Phys. **2**, 323 (2006).

[15] A. Palacios, A. Gonzalez-Castrillo, and F. Martin, Molecular interferometer to decode attosecond electron nuclear dynamics, Proc. Natl. Acad. Sci. U.S.A. **111**, 3973 (2014).

[16] G. De Ninno, B. Mahieu, E. Allaria, L. Giannessi, and S. Spampinati, Chirped Seeded Free-Electron Lasers: Self-Standing Light Sources for Two-Color Pump-Probe Experiments, Phys. Rev. Lett. **110**, 064801 (2013).

[17] E. Allaria *et al.*, Two-colour pump probe experiments with a twin-pulse-seed extreme ultraviolet free-electron laser, Nat. Commun. **4**, 2476 (2013).

[18] T. Hara *et al.*, Two-colour hard x-ray free-electron laser with wide tunability, Nat. Commun. **4**, 2919 (2013).

[19] A. A. Lutman, R. Coffee, Y. Ding, Z. Huang, J. Krzywinski, T. Maxwell, M. Messerschmidt, and H.-D. Nuhn, Experimental Demonstration of Femtosecond Two-Color X-Ray Free-Electron Lasers, Phys. Rev. Lett. **110**, 134801 (2013).

[20] V. Petrillo *et al.*, Observation of Time-Domain Modulation of Free-Electron-Laser Pulses by Multipeaked Electron-Energy Spectrum, Phys. Rev. Lett. **111**, 114802 (2013).

[21] A. A. Lutman *et al.*, Demonstration of Single-Crystal Self-Seeded Two-Color X-Ray Free-Electron Lasers, Phys. Rev. Lett. **113**, 254801 (2014).

[22] E. Roussel, E. Ferrari, E. Allaria, G. Penco, S. Di Mitri, M. Veronese, M. Danailov, D. Gauthier, and L. Giannessi, Multicolor High-Gain Free Electron Laser Driven by Seeded Microbunching Instability Phys. Rev. Lett. **115**, 214801 (2015).

[23] K. C. Prince *et al.*, Coherent control with a shortwavelength free electron laser Nat. Photonics (to be published).

[24] S. A. Rice, New ideas for guiding the evolution of a quantum system, Science **258**, 412 (1992).

[25] V. Blanchet, C. Nicole, M.-A. Bouchene, and B. Girard, Temporal Coherent Control in Two-Photon Transitions: From Optical Interferences to Quantum Interferences, Phys. Rev. Lett. **78**, 2716 (1997).

[26] K. Ohmori, H. Katsuki, H. Chiba, M. Honda, Y. Hagihara, K. Fujiwara, Y. Sato, and K. Ueda, Real-Time Observation of Phase-Controlled Molecular Wave-Packet Interference, Phys. Rev. Lett. **96**, 093002 (2006).

[27] N. A. Kurnit, I. D. Abella, and S. R. Hartmann, Observation of a Photon Echo, Phys. Rev. Lett. **13**, 567 (1964).

[28] *Persistent Spectral Hole-Burning: Science and Applications*, edited by W. E. Moerner (Springer, New York, 1988), Vol. 44.

[29] E. Allaria *et al.*, Highly coherent and stable pulses from the FERMI seeded free-electron laser in the extreme ultraviolet, Nat. Photonics **6**, 699 (2012).

[30] E. Allaria *et al.*, Two-stage seeded soft-x-ray free-electron laser, Nat. Photonics **7**, 913 (2013).

[31] L. H. Yu, Generation of intense UV radiation by subharmonically seeded single-pass free-electron lasers, Phys. Rev. A **44**, 5178 (1991).

[32] G. V. Stupakov, Effect of finite pulse length and laser frequency chirp on HGHG and EEHG seeding, SLAC, 2011.

[33] D. Gauthier *et al.*, Spectrotemporal Shaping of Seeded Free-Electron Laser Pulses, Phys. Rev. Lett. **115**, 114801 (2015).

[34] G. De Ninno *et al.*, Single-shot spectro-temporal characterization of XUV pulses from a seeded free-electron laser, Nat. Commun. **6**, 8075 (2015).

[35] See the Supplemental Material http://link.aps.org/supplemental/10.1103/PhysRevLett.116.024801, which includes Refs. [36,37]: electron beam time-dependent energy profile and its effect on the FEL pulse properties and fringe displacement.

[36] P. Craievich *et al.*, Implementation of radio-frequency deflecting devices for comprehensive high-energy electron beam diagnosis, IEEE Trans. Nucl. Sci. **62**, 210 (2015).

[37] T. Shaftan and L. H. Yu, High-gain harmonic generation free-electron laser with variable wavelength, Phys. Rev. E **71**, 046501 (2005).

[38] M. Zangrando, D. Cocco, C. Fava, S. Gerusina, R. Gobessi, N. Mahne, E. Mazzucco, L. Raimondi, L. Rumiz, and C. Svetina, Recent results of PADReS, the photon analysis delivery and reduction system, from the FERMI FEL commissioning and user operations, J. Synchrotron Radiat. **22**, 565 (2015).

[39] J. Goodman, *Introduction to Fourier Optics* (Robert & Company Publishers, Greenwood Village, CO, 2005).

[40] P. R. Ribič and G. Margaritondo, Status and prospects of x-ray free-electron lasers (X-FELs): A simple presentation, J. Phys. D **45**, 213001 (2012).

[41] G. Penco, M. Danailov, A. Demidovich, E. Allaria, G. De Ninno, S. Di Mitri, W. M. Fawley, E. Ferrari, L. Giannessi, and M. Trovó, Experimental Demonstration of Electron Longitudinal-Phase-Space Linearization by Shaping the Photoinjector Laser Pulse, Phys. Rev. Lett. **112**, 044801 (2014).

[42] T. Shaftan and Z. Huang, Experimental characterization of a space charge induced modulation in high-brightness electron beam, Phys. Rev. ST Accel. Beams **7**, 080702 (2004).

[43] P. Sigalotti, T. Tschentscher, K. Tiedtke, P. Cinquegrana, A. Demidovich, R. Ivanov, I. Nikolov, G. Kurdi, and M. B. Danailov, Ultrafast laser synchronization at the FERMI@Elettra FEL, Proc. SPIE Int. Soc. Opt. Eng. **8778**, 87780Q (2013).

[44] J. Wu, J. B. Murphy, P. J. Emma, X. Wang, T. Watanabe, and X. Zhong, Interplay of the chirps and chirped pulse compression in a high-gain seeded free-electron laser, J. Opt. Soc. Am. B **24**, 484 (2007).

[45] P. R. Ribič, D. Gauthier, and G. De Ninno, Generation of Coherent Extreme-Ultraviolet Radiation Carrying Orbital Angular Momentum, Phys. Rev. Lett. **112**, 203602 (2014).

[46] S. T. Cundif and Y. Jun, Colloquium: Femtosecond optical frequency combs, Rev. Mod. Phys. **75**, 325 (2003).

[47] S. A. Diddams *et al.*, An optical clock based on a single trapped 199 Hg + ion Science **293**, 825 (2001).

[48] C. Leichtle, W. P. Schleich, I. Sh. Averbukh, and M. Shapiro, Quantum State Holography, Phys. Rev. Lett. **80**, 1418 (1998).